CrossMark

Design and Optimization of Composite Automotive Hatchback Using Integrated Material-Structure-Process-Performance Method

Xudong Yang[1,2] · Lingyu Sun[1,2] · Cheng Zhang[1,2] ·
Lijun Li[1,2] · Zongmiao Dai[3] · Zhenkai Xiong[3]

Abstract The application of polymer composites as a substitution of metal is an effective approach to reduce vehicle weight. However, the final performance of composite structures is determined not only by the material types, structural designs and manufacturing process, but also by their mutual restrict. Hence, an integrated "material-structure-process-performance" method is proposed for the conceptual and detail design of composite components. The material selection is based on the principle of composite mechanics such as rule of mixture for laminate. The design of component geometry, dimension and stacking sequence is determined by parametric modeling and size optimization. The selection of process parameters are based on multi-physical field simulation. The stiffness and modal constraint conditions were obtained from the numerical analysis of metal benchmark under typical load conditions. The optimal design was found by multi-discipline optimization. Finally, the proposed method was validated by an application case of automotive hatchback using carbon fiber reinforced polymer. Compared with the metal benchmark, the weight of composite one reduces 38.8%, simultaneously, its torsion and bending stiffness increases 3.75% and 33.23%, respectively, and the first frequency also increases 44.78%.

✉ Lijun Li
  lilijun@buaa.edu.cn

[1] School of Transportation Science and Engineering, Beihang University, 37 Xueyuan Road, Haidian District, Beijing 100191, China

[2] Lightweight Vehicle Innovation Center, Beihang University, 37 Xueyuan Road, Haidian District, Beijing 100191, China

[3] The 713 Research Institute of China Shipbuilding Industry Corporation, Zhengzhou, Henan 450015, China

🍎 Springer

1 Introduction

Fiber-reinforced polymer composite are gradually being widely used in automotive industry with its excellent performance and lighter weight compared with steel. However, it is difficult to predict the component performance because it is dependent on the material properties, structural design and manufacturing process which restrict mutually. Additionally, the anisotropy of material and simultaneous formability of structure and material increase the difficulty of integrated design.

The relationships between performance and other three factors, materials [1–3], structure [4, 5] and manufacturing process [6–8], have been studied separately. But the influence of a certain factor alone on performance neglect the interaction among these four factors in the design process [9, 10], which increase the number of infeasible designs and optimization iteration so that the cycle of design is extended. Therefore, there is an urgent need for an integrated design method combining these four factors together.

Currently, some scholars are trying to solve this problem by two methods, namely, multi-disciplinary design optimization (MDO) and knowledge based engineering (KBE). For example, Grujicic et al. [11] applied MDO methodology to develop a composite inner door panel using a specific material. In a previous work [12], MDO was applied this to automotive composite components. However, MDO method determines the structure and manufacturing process parallelly, ignoring the interactions of structure design, process analysis and performance, which increases the number of infeasible designs. Wang et al. [13] and Choi et al. [14] performed cost/weight optimizations based on KBE at conceptual design stage. However, the KBE needs large numbers of engineering cases and method to construct the knowledge base, not suitable for a new design.

This paper aims to propose an integrated method and provide theoretical basis and technical guidance for the design and production of composite laminate components. The feasibility of this method will be verified by the design and optimization of an automotive hatchback using carbon fiber polymer composite.

In this paper, the method of integration, which is the core of this paper, is firstly introduced in Section 2.1, followed by Section 2.2 introducing the theory of each part in this integration design. A case of an automotive hatchback is used to verify the feasibility of this integration method in Section 3. Section 3.1 analyzes the benchmark performance and Section 3.2 is the integration design of composite hatchback, in which the material selection, structure design, process analysis and performance evaluation are introduced in Section 3.2.1-3.2.4 corresponding to the theory part in Section 2.2.1-2.2.4. Finally, Section 4 summarizes the key conclusions resulting from the present study.

2 Methodology and Theory

2.1 Method of Integration

The design flow chart of integrated material-structure-process-performance design is shown in Fig. 1.

It is divided into four parts: material selection, structure design, process simulation and performance verification. The performances of original metal component obtained from CAD/CAE model are taken as constraint conditions to optimize the other three factors.
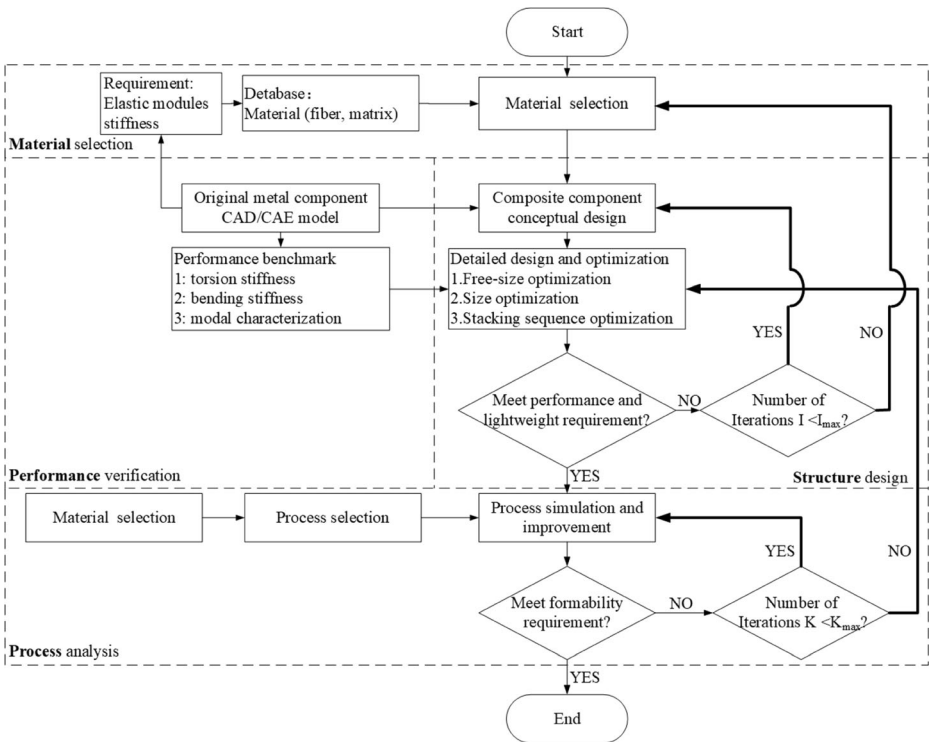
Fig. 1 Flow chart of integration optimization method

Design synthesis starts with the material selection, which is taken as the highest priority due to the changes of material in actual production, will bring increasing costs and time of trial and errors. Therefore, the first step is to select an appropriate material from the material database under the requirements of elastic modules and stiffness, some of which have been verified practically. In order to ensure the accuracy of design, as well as to avoid these multiple performance requirements being in conflict [15], some iteration loops are included.

As for structure design, based on the existing metal component, some restrict conditions on geometrical shapes and installation space of the composite component is determined. At the same time, the mechanical properties such as bending stiffness, torsion stiffness and the first-order constrained frequency of the metal components are taken as performance constraints and weight reduction is taken as the objective to optimize the structural design of composite components, including free-size optimization, size optimization, and stacking sequence optimization. If not satisfied the performance and weight requirements after optimization, then return to change the conceptual design of composite components when the number of iterations, I, is less than the maximum number of iterations, I_{max}. Otherwise, material and process need to be changed.

As for process analysis, some process parameters such as the air traps and the cropping angle related to formability are checked. If meet the manufacturing requirements, the design process is completed. If not satisfied, return to adjust the process parameters when the number

of iterations K is less than the maximum number of iterations K_{max}, otherwise detailed design may need to be changed using optimization method.

The basic theory of each part in this integrated approach are followed below.

2.2 Theory of Integration Design

2.2.1 Material Selection

Most studies concerned with the evaluation of mechanical behavior of fiber reinforced composites use what is called a "Rule-Of-Mixtures" (hereafter designated as ROM) to predict and/or to compare the strength and stiffness properties of the composites [16]. The ROM is an operational tool that uses weighted volume average of the component properties in isolation to obtain the magnitude of the property for the composite. Specifically, in the case of composite containing uniaxially aligned, continuous fibers, the composite stress is written as [16]

$$\sigma_c = \sigma_f V_f + \sigma_m V_m \tag{1}$$

where σ is the axial stress, V is the volume fraction of the component and the subscripts c, f and m refer to the composite, fiber and matrix, respectively. It is to be noted that $V_f + V_m = 1$ if the interface phase are neglected.

ROM relationship for the longitudinal elastic modulus is as follows

$$E_1 = E_f V_f + E_m V_m \tag{2}$$

ROM the transverse elastic modulus is as follows

$$E_2 = \frac{E_f E_m}{V_m E_f + V_f E_m} \tag{3}$$

2.2.2 Structure Design

Design optimization means the possibility of producing the best design while meeting all constraints. Composite laminate optimization technology takes the formability into account, imposes non-mandatory manufacturing constraints at the conceptual design stage of free-size optimization and imposes more detailed manufacturing constraints at the detailed design stage of the cascading order optimization. OptiStruct-based composite structure optimization process consists of three main stages: free size optimization, ply-based sizing optimization and stacking sequence optimization.

(1) Free size optimization

The purpose of composite free-sizing optimization is to create design concepts that utilize all the potential of a composite structure where both structure and material can be designed simultaneously. By varying the thickness of each ply with a particular fiber orientation for every element, the total laminate thickness can change 'continuously' throughout the structure, and at the same time, the optimal composition of the composite laminate at every point (element) is achieved simultaneously.

The mathematical model of structural optimization design [17, 18] can be expressed as follows:

$$\text{Minimize the objective function}: f(x)$$
$$\text{Constraints}: g_i(x) - g_j^u \leq 0, j = 1...M$$
$$x_{i\kappa}^L \leq x_{i\kappa} \leq x_{i\kappa}^U, i = 1...N_p, \kappa = 1...NE$$

$f(x)$ represents the objective function, $g_i(x)$ and g_j^u represents the j-th constraint response and the upper limit of the response, respectively. M indicates the number of all constraints. NE indicates the number of cells, N_p is the number of super-layers, X_{ik} represents the thickness of the i-th super-layer where the first cell is located.

The formula above is the free size formula. As Fig. 2 shows, in the free-size optimization, a super-ply concept should be adopted, in which each available fiber orientation is assigned a super-ply whose thickness is free-sized. In other words, a super-ply is the total designable thickness of a particular fiber orientation. Moreover, manufacturing constraints also need to be set, such as the percentage of each ply angle in total thickness, the total thickness of the laminate and so on. This stage considers only the global response and non-mandatory manufacturing constraints. The manufacturing constraints of the total thickness and the percentage of monolayer thickness are described mathematically as follows:

$$\text{Total thickness}: T_\kappa^L \leq \sum x_{i\kappa} \leq T_\kappa^U \, \kappa = 1...NE$$
$$\text{Monolayer thickness percentage}: P_j^L \leq \frac{x_{jk}}{\sum\limits_{j=1}^{N_P} x_{ik}} \leq P_j^U \, j = 1...NE$$

where T_κ^L and T_κ^U represent the lower and upper laminate thickness limits respectively, P_j^L and P_j^U represent the lower and upper percentages of monolayer thickness percentages respectively.

(2) Ply-based sizing optimization

The result of the free size optimization is that a corresponding continuous thickness distribution is generated for each fiber direction. Each thickness has several layers, each layer represents a multi-layer combination of the same direction. Experience shows that there being four layers in each fiber direction could provide a good balance between the trueness of the thickness and the complexity of the shape. The different layers stack together to form the
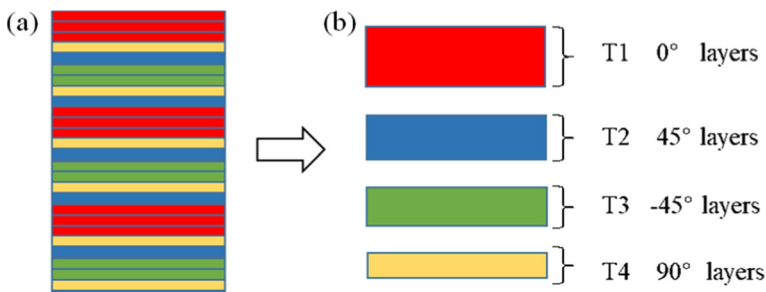

Fig. 2 Super-ply concept in free size optimization: **a** Initial ply **b** Super-ply

laminate. The mathematic model of the size optimization is the same as the free size optimization, but the design variables are discrete thicknesses that increase in base thickness.

(3)   Stacking sequence optimization

Composite plies are shuffled to determine the optimal stacking sequence for the given design optimization problem while also satisfying additional manufacturing constraints. Stacking sequence optimization aims to evaluate a huge number of stacking combinations from both performance and manufacturability perspectives. After the completion of size optimization, all details of layers have been completed, but the detailed manufacturing constraints may not be satisfied. In this phase, the stacking sequence is optimized for all layers subject to all design constraints.

2.2.3 Process Analysis

Based on the volume averaging techniques, Darcy's law [19] is often used to model the resin flow through porous media. It establishes a relationship between the average fluid velocity $\langle \overline{\nu}_r \rangle$ and the pressure gradient ∇P:

$$\left\langle \overline{\nu}_r \right\rangle = -\frac{[K]}{\varphi \mu_r} \langle \nabla P \rangle \tag{4}$$

where $[K]$ is the permeability tensor, μ_r the resin viscosity and ϕ the porosity of the porous medium (fibrous reinforcement).

Assuming that the reinforcement is not a deformable medium, the following equation of mass conservation may be considered:

$$div\left(\frac{[K]}{\mu_r} \langle \nabla P \rangle\right) = 0 \tag{5}$$

Castro-Macosko model [20] is used to predict the viscosity variations due to resin conversion that may occur during impregnation.

To model heat transfer, the whole system including the mold, resin and fibrous reinforcement is considered. The lumped approximation assumes that the fibers and the surroundings fluid are at an average temperature. Following this approach any averaged physical property may be estimated by the rule of mixture, based on the mass fractions of the lumped components. In the case of dominant convection, the heat balance equation includes a source term $f(T)$ arising from the heat generated by resin polymerization. Therefore it is written in the following form:

$$\frac{\partial T}{\partial t} + \overline{\nu} \cdot \nabla T = f(T) \tag{6}$$

At the flow front, a Dirichlet boundary condition may be imposed based on the temperature of the dry fibrous reinforcement or a flux boundary condition is derived by a backwind approximation to estimate the heat transferred by the incoming resin. At the interface between Neglecting species diffusion, the mass balance can be expressed as:

$$\phi \frac{\partial \alpha}{\partial t} + \overline{\nu} \cdot \nabla \alpha = \phi \dot{H} \tag{7}$$

where $\dot{H}$ is the rate of heat generated by resin polymerization. Reaction kinetics is usually describes by Kamal-Sorour [21] model.

Based on the process simulation, the formability is validated numerically.

2.2.4 Performance Verification

The mechanical behavior of composite components could be derived using the principle of composite mechanics for continuous fiber-reinforced laminate.

For a composite component, the principle of equal stiffness design can be adopted. Consider an individual layer k in a multidirectional laminate whose midplane is at a distance Z_k from the laminate reference plane. The stress-strain relations for this layer referred to its material axes are as follows in brief [22],

$$[\sigma]_{x,y}^\kappa = [Q]_{x,y}^\kappa [\varepsilon^0]_{x,y} + z[Q]_{x,y}^\kappa [\kappa]_{x,y} \tag{8}$$

These relations about laminates can be obtained,

$$\begin{bmatrix} N_x \\ N_y \\ N_z \end{bmatrix} = \sum_{\kappa=1}^{n} \left\{ \begin{bmatrix} Q_{xx} & Q_{xy} & Q_{xs} \\ Q_{yx} & Q_{yy} & Q_{ys} \\ Q_{sx} & Q_{sy} & Q_{ss} \end{bmatrix} \begin{bmatrix} \varepsilon_x^0 \\ \varepsilon_y^0 \\ \gamma_s^0 \end{bmatrix} \int_{h_{\kappa-1}}^{h_\kappa} dz + \begin{bmatrix} Q_{xx} & Q_{xy} & Q_{xs} \\ Q_{yx} & Q_{yy} & Q_{ys} \\ Q_{sx} & Q_{sy} & Q_{ss} \end{bmatrix} \begin{bmatrix} \kappa_x^0 \\ \kappa_y^0 \\ \kappa_s^0 \end{bmatrix} \int_{h_{\kappa-1}}^{h_\kappa} z dz \right\} \tag{9}$$

And

$$\begin{bmatrix} M_x \\ M_y \\ M_z \end{bmatrix} = \sum_{\kappa=1}^{n} \left\{ \begin{bmatrix} Q_{xx} & Q_{xy} & Q_{xs} \\ Q_{yx} & Q_{yy} & Q_{ys} \\ Q_{sx} & Q_{sy} & Q_{ss} \end{bmatrix} \begin{bmatrix} \varepsilon_x^0 \\ \varepsilon_y^0 \\ \gamma_s^0 \end{bmatrix} \int_{h_{\kappa-1}}^{h_\kappa} dz + \begin{bmatrix} Q_{xx} & Q_{xy} & Q_{xs} \\ Q_{yx} & Q_{yy} & Q_{ys} \\ Q_{sx} & Q_{sy} & Q_{ss} \end{bmatrix} \begin{bmatrix} \kappa_x^0 \\ \kappa_y^0 \\ \kappa_s^0 \end{bmatrix} \int_{h_{\kappa-1}}^{h_\kappa} z^2 dz \right\} \tag{10}$$

In the expressions above, the stiffness $[Q]_{x,y}^\kappa$, reference plane strains $[\varepsilon^0]_{x,\ y}$, and curvatures $[\kappa]_{x,\ y}$ are taken outside the integration operation since they are not functions of z. Of these quantities only the stiffnesses are unique for each layer, whereas the reference plane strains and curvatures refer to the entire laminate and are the same for all piles. Thus $[\varepsilon^0]_{x,\ y}$ and $[\kappa]_{x,\ y}$ can be factored outside the summation sign as follows [21]:

$$[N]_{x,y} = \left[\sum_{\kappa=1}^{n} [Q]_{x,y}^\kappa \int_{h_{\kappa-1}}^{h_\kappa} dz \right] [\varepsilon^0]_{x,y} + \left[\sum_{\kappa=1}^{n} [Q]_{x,y}^\kappa \int_{h_{\kappa-1}}^{h_\kappa} z dz \right] [\kappa]_{x,y} \tag{11}$$

$$[M]_{x,y} = \left[\frac{1}{2} \sum_{\kappa=1}^{n} [Q]_{x,y}^\kappa (h_\kappa^2 - h_{\kappa-1}^2) \right] [\varepsilon^0]_{x,y} + \left[\frac{1}{3} \sum_{\kappa=1}^{n} [Q]_{x,y}^\kappa (h_\kappa^3 - h_{\kappa-1}^3) \right] [\kappa]_{x,y} \tag{12}$$

$$[N]_{x,y} = [A]_{x,y} [\varepsilon^0]_{x,y} + [B]_{x,y} [\kappa]_{x,y} \tag{13}$$

$$[M]_{x,y} = [B]_{x,y} [\varepsilon^0]_{x,y} + [D]_{x,y} [\kappa]_{x,y} \tag{14}$$

where

$$A_{ij} = \sum_{\kappa=1}^{n} Q_{ij}^{\kappa}(h_{\kappa}-h_{\kappa-1}) \tag{15}$$

$$B_{ij} = \frac{1}{2} \sum_{\kappa=1}^{n} Q_{ij}^{\kappa}\left(h_{\kappa}^2-h_{\kappa-1}^2\right) \tag{16}$$

$$D_{ij} = \frac{1}{3} \sum_{\kappa=1}^{n} Q_{ij}^{\kappa}\left(h_{\kappa}^3-h_{\kappa-1}^3\right) \tag{17}$$

with $i, j = x, y, s$.

Thus, in full form the force-deformation relations are as follows:

$$\begin{bmatrix} N_x \\ N_y \\ N_z \end{bmatrix} = \begin{bmatrix} A_{xx} & A_{xy} & A_{xs} \\ A_{yx} & A_{yy} & A_{ys} \\ A_{sx} & A_{sy} & A_{ss} \end{bmatrix} \begin{bmatrix} \varepsilon_x^0 \\ \varepsilon_y^0 \\ \gamma_s^0 \end{bmatrix} + \begin{bmatrix} B_{xx} & B_{xy} & B_{xs} \\ B_{yx} & B_{yy} & B_{ys} \\ B_{sx} & B_{sy} & B_{ss} \end{bmatrix} \begin{bmatrix} \kappa_x \\ \kappa_y \\ \kappa_s \end{bmatrix} \tag{18}$$

And the moment-deformation relations are as follows:

$$\begin{bmatrix} M_x \\ M_y \\ M_z \end{bmatrix} = \begin{bmatrix} B_{xx} & B_{xy} & B_{xs} \\ B_{yx} & B_{yy} & B_{ys} \\ B_{sx} & B_{sy} & B_{ss} \end{bmatrix} \begin{bmatrix} \varepsilon_x^0 \\ \varepsilon_y^0 \\ \gamma_s^0 \end{bmatrix} + \begin{bmatrix} D_{xx} & D_{xy} & D_{xs} \\ D_{yx} & D_{yy} & D_{ys} \\ D_{sx} & D_{sy} & D_{ss} \end{bmatrix} \begin{bmatrix} \kappa_x \\ \kappa_y \\ \kappa_s \end{bmatrix} \tag{19}$$

The expressions above can be combined into one general expression relating in-plane forces and moments to reference plane strains and curvatures [22].

$$\begin{bmatrix} N \\ M \end{bmatrix} = \begin{bmatrix} A & B \\ B & D \end{bmatrix} \begin{bmatrix} \varepsilon^0 \\ \kappa \end{bmatrix} \tag{20}$$

The relationships above are expressed in terms of three laminate stiffness matrices $[A]$, $[B]$ and $[D]$, which are functions of the geometry, material properties and stacking sequence of the individual plies. They are the average elastic parameters of the multidirectional laminate with the following significance:

A_{ij} are extensional stiffnesses, or in-plane laminate moduil, relating in-plane loads to in-plane strains.

B_{ij} are coupling stiffnesses, or in-plane/flexure coupling laminate moduil, relating in-plane loads to curvatures and moments to in-plane forces produce flexural and twisting deformations; moments produce extension of the middle surface in addition to flexure and twisting.

D_{ij} are bending or flexural laminate stiffnesses relating moments to curvatures.

In numerical analysis of performance, the residual stress from the manufacture process and actual fiber direction could be considered in integrated design through data transfer between different softwares.

3 Case Study: Design and Optimization of Composite Automotive Hatchback

3.1 Benchmark Performance Analysis

In this section, the performance of original steel hatchback will be calculated by finite element method, which will be taken as the constraint condition in the preliminary design of composite hatchback.

The steel hatchback model used in this verification is derived from a SUV vehicle. The material properties of DP 590 steel used in the hatchback are as follows: the destiny is 7850 kg/ m^3, the elastic modulus is 207 GPa and the poisson's ratio is 0.3. Figure 3 shows the CAD model of steel hatchback, which consists of inner panel, outer panel and other bearing parts, as well as window reinforcement panel, lock assembly and other additional components. They are made of different thickness of stamping steel panels and welded together.

The thickness of each part is listed in the Table 1.

In the finite element pre-processing software Hypermesh™, the DP 590 steel hatchback model is simplified and geometrically cleaned, and the components are meshed by shell elements. The FE model of steel hatchback is shown in Fig. 4. The total mass is 12.26 kg.

The global unit size of the finite element model is 3 mm, with 202,725 nodes, 202,408 elements. The number of triangular elements is less than 1%. As shown in Table 2, the convergence of finite element model was verified by deflections under bending conditions.

The stiffness performance of steel hatchback under the torsion and bending conditions, as well as first-order restraint frequency and modal shape are analyzed and evaluated. The description of loading condition and constraint conditions are shown in Table 3.
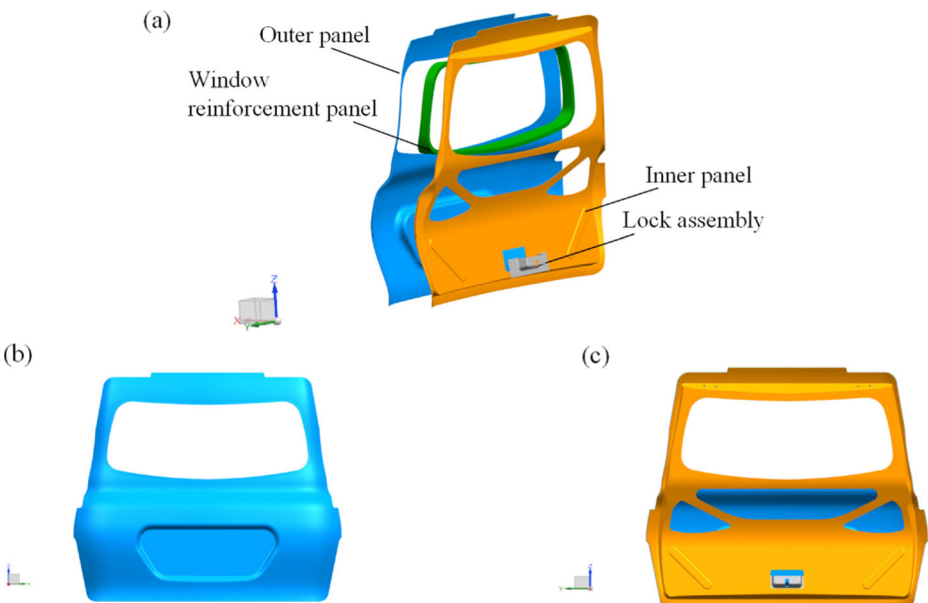

Fig. 3 Original DP 590 steel hatchback CAD model: a exploded view b front view c rear view

Table 1 The thickness of each part in DP 590 steel hatchback system

Part	Thickness (mm)
Inner panel	0.8
Outer panel	0.6
Window reinforcement panel	2
Lock assembly	1.5

The torsion stiffness is indicated by the maximum torsion angle at the load application position, which is calculated by the maximum displacement divided by wheelbase. The bending stiffness is indicated by bending deflection. The vibration performance is evaluated by the first-order modal frequency. The results are listed in Table 4, which will be used as a baseline for optimizing the composite hatchback. The corresponding displacement contours are shown in Fig. 5.

3.2 Integration Design of Composite Hatchback

3.2.1 Material Selection

The material used for inner and outer panel is the carbon fiber-reinforced epoxy composite, which has high specific strength and stiffness. With the progress of large-tow carbon fiber and spreading technology, the cost of carbon fiber composite is also greatly reduced, gradually applied to the automotive industry. In our design, the carbon fiber is PANEX33-48 k from Zoltek Company, and the resin is 5222B from Institute of Aeronautical materials.

3.2.2 Structure Design

In this section, the conceptual design, detailed design and optimization of the composite hatchback are carried out. The free-size optimization, size optimization and stacking sequence optimization of the composite hatchback are set to further enhance the lightweight.
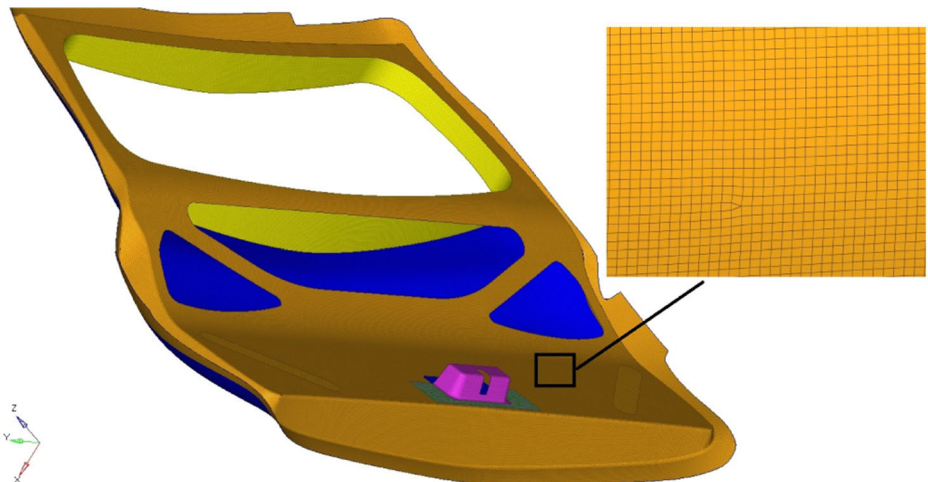
Fig. 4 Finite element model of DP 590 steel hatchback

Table 2 The convergence of FE model

Global unit size (mm)	10	5	3	2	1
Deflection (mm)	0.941	0.820	0.710	0.700	0.700

(1) Conceptual design of composite hatchback

According to the theory of composite mechanics [22], the stiffness of a typical laminate can be expressed as follows:

$$\begin{bmatrix} N \\ M \end{bmatrix} = \begin{bmatrix} A & B \\ B & D \end{bmatrix} \begin{bmatrix} \varepsilon^0 \\ \kappa \end{bmatrix} \tag{21}$$

where N matrix is the internal force on the cross section of the laminate; M matrix is the internal torque on the cross section of the laminate; ε_0 is midplane strain of laminate; κ is midplane curvature and twist of laminate. Matrix A only includes internal force and midplane-related stiffness coefficient, collectively referred to as tensile stiffness matrix. Matrix D is the stiffness coefficient associated with the moment and curvature and the twist rate. Matrix B characterizes the coupling between bending and tensile, collectively referred to as coupling stiffness matrix.

$$[B] = B_{ij} = \frac{1}{2} \sum_{\kappa-1}^{n} \left(\overline{Q_{ij}} \right)_{\kappa} \left(z_{\kappa}^2 - z_{\kappa-1}^2 \right) \tag{22}$$

Table 3 Loading and constraint conditions for performance evaluation
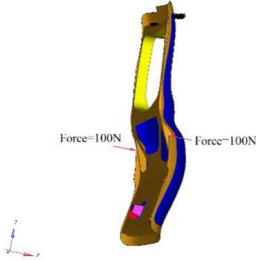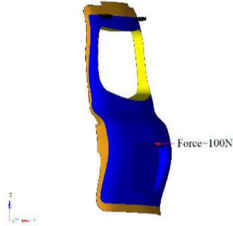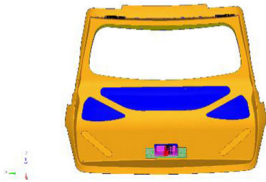
No.	FE model	Constraints and loads	Performance
1	Force=100N — Force=100N	Restricts: ● All DOFs at hinge ● Translation DOFs at lock Loading: ● A pair of reverse forces	Torsion stiffness
2	Force=100N	Restricts: ● All DOFs at hinge ● Translation DOFs at Loading: ● Normal loading at center	Bending stiffness
3		Restricts: ● All DOFs at hinge ● Translation DOFs at lock ● No loads	Vibration frequency

Table 4 Reference design constraints obtained from DP 590 steel hatchback

Subcase target	Value
Torsion angle (°)	0.133
Bending deflection (mm)	0.710
1st modal frequency (Hz)	27.4

Symmetrical laminates are symmetrical about the geometrical dimensions and material properties.

$$\left(\overline{Q_{ij}}\right)_1 = \left(\overline{Q_{ij}}\right)_n \tag{23}$$

$$\left(z_1^2 - z_0^2\right) = -\left(z_n^2 - z_{n-1}^2\right) \tag{24}$$

Substituting Eq. (21), the following equation can be got.

$$[B] = B_{ij} = 0 \tag{25}$$

B = 0 means that there is no coupling between the in-plane and the outside, and the in-plane tensile compression has no coupling relationship with the outward bending. This can avoid uncontrollable deformation, but also similar to the isotropic steel hatchback, so we can use the symmetrical laminates for the initial layup.

When replacing steel with continuous fiber composites, it is necessary to perform an initial layup design of the laminate. The unidirectional tape mechanical properties are shown in the Table 5. The thickness of single layer is 0.125 mm. The ply angles which commonly used in engineering are 0°, 90°, 45°and −45°.

The thickness of the laminate is directly related to performance and weight. Existing automotive composite parts, such as doors, engine covers and trunk covers. The thickness is generally between 1.2–2 mm. For safety reason, the conservative will be tentatively set to 2 mm, same in the inner and outer panel. Taking into account the hatchback is the semi-structural parts,
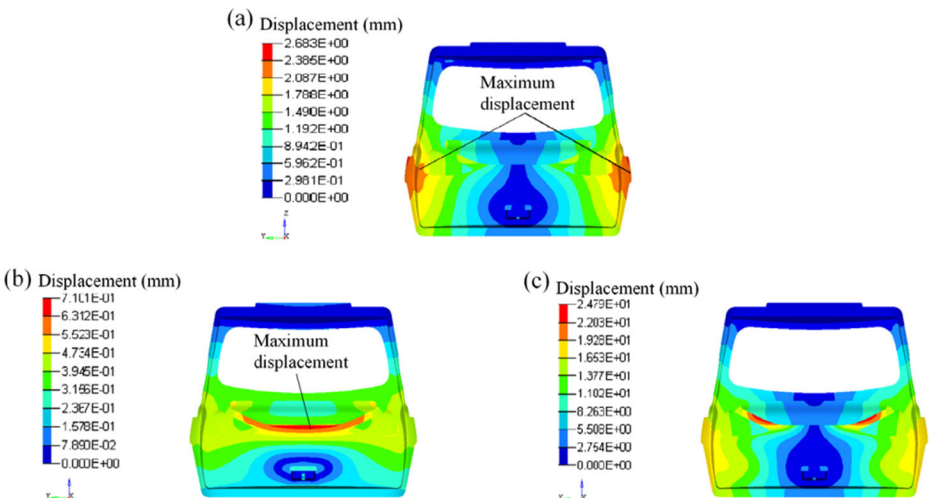

Fig. 5 Displacement contour of DP 590 steel hatchback: **a** torsion **b** bending **c** constraint modal analysis

Table 5 Unidirectional tape mechanical properties

Parameters	Value
Longitudinal elastic modulus (GPa)	130
Transverse elastic modulus (GPa)	9.6
In-plane Possion's ratio	0.338
Shear modulus (GPa)	4.51
Density (kg/m^3)	1600
Single layer thickness (mm)	0.125

but also the appearance of pieces, may be subject to a variety of load. So the layup of the various directions should be uniform, in order to bear the load in different directions.

Based on the analysis above, the initial layup is selected as [0, 0, 45, 45, 90, 90,-45,-45]$_s$, symmetric laying. The total thickness is 2 mm with 16 layers. In this substitution, only the material of the inner and outer panel is replaced by steel into composite laminate, the geometry of which and other components being temporarily unchanged.

The response of the initial composite hatchback is analyzed with the same subcases as the steel one. Figure 6 shows the results, in which the contours are similar to the steel hatchback. However, the first-order constraint mode of composite hatchback is asymmetric torsional mode shape instead of local bending. It may be caused by the orthotropic or other directional coupling effects of the fiber reinforced composite [23–25].

Table 6 shows the performance comparison between the DP 590 steel hatchback and the initial composite hatchback. It can be seen that the weight of the initial composite hatchback is significantly reduced, but the performance is still redundant comparing to the steel one and has a lot of room for optimization.

(2)   Detailed design and optimization of composite hatchback

The SUV hatchback can be subject to various types of loads, such as bending, twisting, sagging, road and engine vibration, even crashing, etc. Common loads, such as pushing by
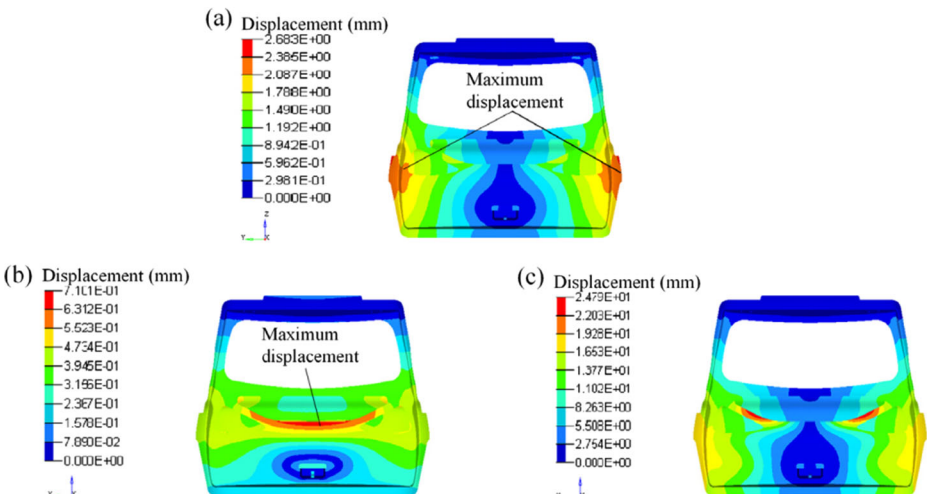

Fig. 6 Displacement contour of composite hatchback: **a** torsion **b** bending **c** constraint modal analysis

Table 6 Comparison between DP steel and composite hatchback

Parameters	Steel hatchback	Composite hatchback (initial)	Percent of change
Weight (kg)	12.26	8.55	−30.26%
Torsion angle (°)	0.133	0.069	−48.12%
Bending deflection (mm)	0.710	0.406	−42.82%
1st modal frequency (Hz)	27.4	45.9	+56.57%

hands, some dangerous like rear-end collision, all have high demands on the bending resistance of the hatchback. Designers are more concerned about bending subcase. Therefore, free-size optimization will be carried out in this step to obtain the ideal material distribution on the bending performance of inner and outer panel.

In order to construct an optimized finite element model, it is necessary to make some adjustments to the initial composite finite element model. On the one hand, the shape of inner panel is based on the topography and topology optimization results of steel bringing the ribs and lighting holes, which need to be removed. On the other hand, thickness and stacking sequence of laminates are unknown, so according to the super-layer theory introduced above. Ignoring the stacking sequence, the layers which have same ply angle are defined as a 'Super ply' and the number of 'Super plies' is only relevant to the number of ply angles. Hence, the initial composite laminate can be simplified as 4 'Super-plies' of 0°,45°,90°and −45°. The thickness of each 'Super plies' is 0.5 mm. In order to avoid torsional stress caused by asymmetry of ±45 ° layers, a ±45 ° lay-up balance constraint is imposed. The optimization function is as below.

Design variables:	Thickness of each 'Super ply' in every shell element
Design constraints:	Volume fraction<0.3
	±45° layers in balance
	Minimum thickness≥0.125 mm
Design objective:	Minimum compliance in separate bending subcase

Figures 7 and 8 show the thickness distribution of inner and outer panel. The bending load transfer path can be seen clearly. The results will be the reference for subsequent system design.
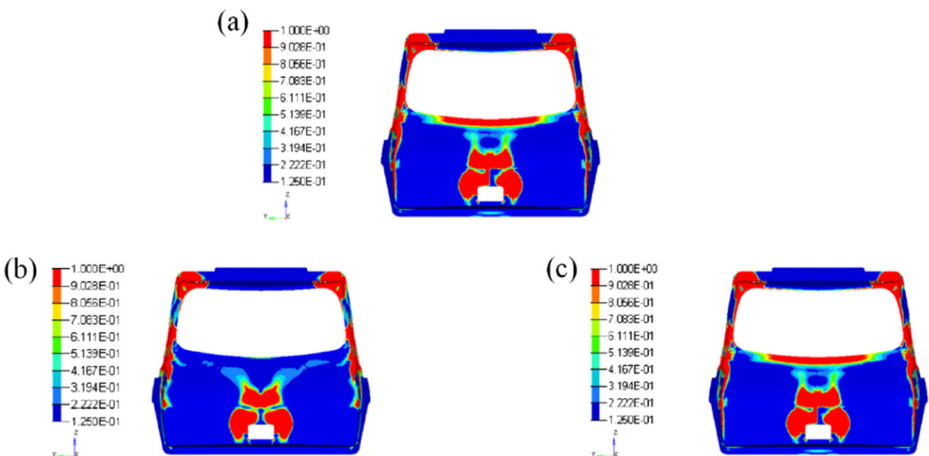

Fig. 7 'Super plies' thickness distribution of inner panel **a** 0° **b** ±45° **c** 90°
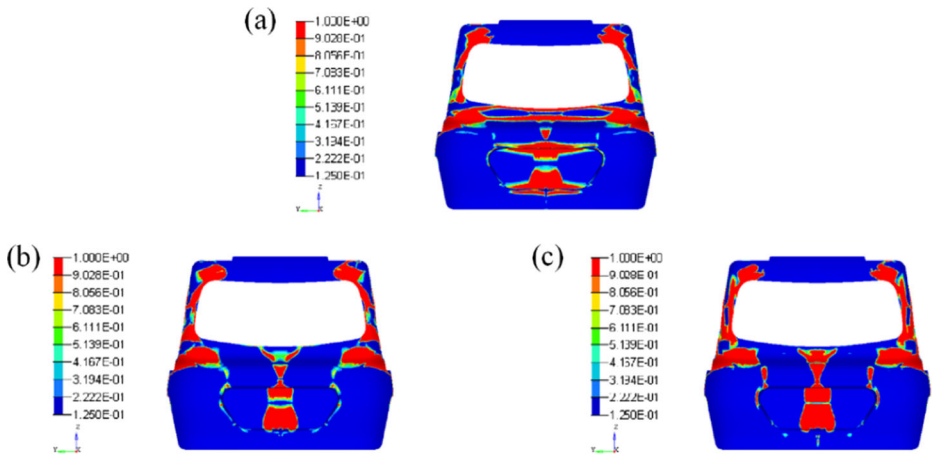
Fig. 8 'Super plies' thickness distribution of outer panel **a** 0° **b** ± 45° **c** 90°

In addition to bending performance, the replacement SUV hatchback also needs to meet the requirements of the other two subcases. At the same time, the thickness distribution obtained from the conceptual design is the optimal solution of the free-size optimization, but the overly complex shape obviously does not meet the process requirements and needs to be reasonably simplified and partitioned. Combined with the conceptual design and the actual size of the carbon fiber cloth, the panels are divided into different zones, in which the shapes of 'Super plies' are the same. Zones division results and names are shown in different colors in Fig. 9.

The thickness of each zone is directly related to the weight, while the hatchback assembly must meet the baseline performance requirements of the steel hatchback. So in size optimization, the performance of the hatchback assembly rather than the inner and outer panel alone should be considered. What's more, since the thickness of the single layer composite is 0.125 mm, size optimization variables are discrete, and are multiples of 0.125. The optimization function is as below.

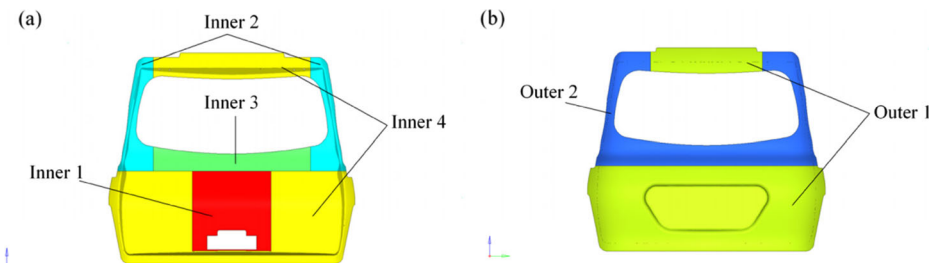|	
Design variables:	Thickness of each 'Super ply' in every zone.
Design constraints:	Subcase 1: angle<baseline
	Subcase 2:defl<baseline
	Subcase 3:freq>baseline
	Move limit = 0.125
	Thickness of each 'Super ply':0.125 mm≤t≤1 mm
Design objective:	Minimum mass of hatchback assembly

Fig. 9 Zones division results **a** inner panel **b** outer panel

Table 7 Thickness of each 'Super ply' in hatchback

Thickness (mm)	0°	±45°	90°
Inner 1	0.25	0.25	0.25
Inner 2	0.375	0.375	0.375
Inner 3	0.25	0.25	0.25
Inner 4	0.5	0.5	0.5
Outer 1	0.5	0.5	0.5
Outer 2	0.5	0.375	0.25

Table 7 shows the thickness of 'Super ply' in every zone. Discretizing each 'Super-ply' in accordance with the thickness of single layer, the number of layers in each layup angle can be obtained. The mass of optimized hatchback is 7.50 kg, which is smaller than initial composite hatchback model. After size optimization, the shape, thickness, and the number of layers in each layup angle of the composite hatchback have been determined.

The overall properties of the composite structure will vary with the stacking sequence of the laminates. We have known that general laminates may produce coupling effects, resulting in uncontrollable deformation. What's more, some other factors should be considered in defining the stacking sequence. If the layers with same ply angle laying continuously too much, delamination may be easily caused [26]. In order to guarantee the beauty and continuity on the surface, the layers on the top and bottom surface in each zone should better be consistent, 45° selected in this paper. The optimization function is as below.

Design variables:	Stacking sequence in each zone
Design constraints:	Symmetry constraint
	45° on the top and bottom
	'Maximum number of successive plies' = 4
Design objective:	Minimum compliance in subcase 2

Table 8 shows the iteration process in zone Inner 1. After 6 iterations, the stacking sequence results can be determined. At this time, all the laminate parameters of the inner and outer panel have been identified.

3.2.3 Process Analysis

In this section, the process of forming the composite hatchback with RTM process will be discussed. The influence of different import and export factors on the forming time and forming quality in filling stage will be analyzed.

The hatchback is one of large panel and shell parts on the body, which the quality and efficiency of the forming process has a high demand. In RTM resin flow filling stage, injection
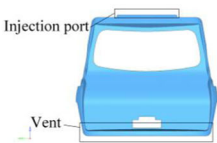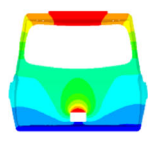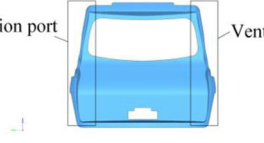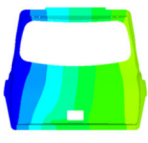
Table 8 Stacking sequence in hatchback
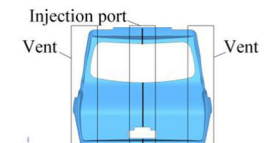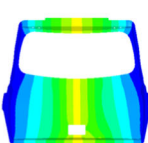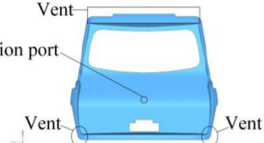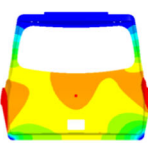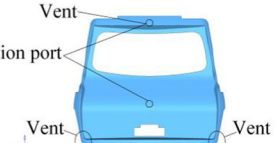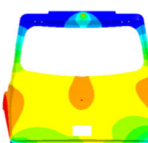
Zone	Stacking sequence
Inner 1	[45,-45,0,90]$_s$
Inner 2	[45,90,-45,45,0,0]$_s$
Inner 3	[45,0,-45,90]$_s$
Inner 4	[45,0,0,-45,45,-45,90,90]$_s$
Outer 1	[45,90,90,-45,-45,45,0,0]$_s$
Outer 2	[45,90,-45,45,0,0]$_s$

Table 9 Parameters used in process simulation

Fiber parameters			
Fiber density (kg/m^3)		Porosity	Permeability (m^2)
1800		0.64	1.1×10^{-11}
Resin parameters		Injection process parameters	
Viscosity (Pa·s) (300 °C)	Resin density (kg/m^3)	Melt temperature (°C)	Pressure (MPa)
0.3	1300	300	1×10^5

pressure, filling temperature, as well as injection port, vent size, location and other import and export factors have a great impact on the filling process [27]. According to the engineering practice, five kinds of filling programs are proposed, and the forming efficiency and quality are determined by comparing the filling time and air-trap distribution of various programs. The parameters used in process simulation are shown in Table 9.

Table 10 Filling time and pressure distribution of 5 alternative programs

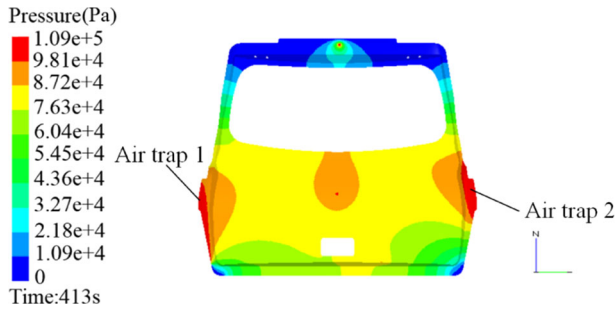| Program	Description	Pressure distribution	Filling time/s
1			1516
2			1367
3			435
4			2607
5			413

Fig. 10 Air traps in Program 5

Programs 1–3 are line injection method, respectively, injecting from top side and exiting from bottom side, injecting from left side and exiting from right side, injecting from center line and exiting from double sides. Programs 4, 5 are point injection methods, single injection at midpoint and two-point injection along the center line.

Using the process simulation software for resin filling process analysis, filling time and ending pressure can be recoded. Some preliminary conclusion can be obtained. Table 10 shows the five alternative programs and pressure distribution, filling time of each program.

In contrast to Programs 1, 2, 3, it is known that when choose line injection, the central axis injection is injected with a shorter flow path than the top side injection and the left side injection, so the time is also greatly reduced. Hence, when selecting the position of the injection port, it should be arranged near the center line. The injection position of Program 4, 5 is on the center line, and the line injection is more efficient than the single point injection, but the two-point injection and the line injection have close injection efficiency. Taking into account the actual production, most of the RTM injection machines are for the single point injection. It is difficult to achieve the function of line injection. When filling time is close, point injection is of top priority. Program 5 is better than others.

Efficiency and quality are two important indicators of the process, so the quality of forming also needs to be guaranteed. Air trap is one of the important factors that affect the quality of forming. Air trap is due to the cavity of the gas is not completely discharged and occupy a certain volume after curing, which seriously affects the aesthetic and performance of the work piece and need to avoid [28]. By properly setting the position, number and size of vents can prevent the appearance of the air trap.

Figure 10 shows the air traps in Program 5. In pressure contour of Program 5, the vent is located at the upper side and lower corner of the hatchback, consistent with the low pressure area. However, except for injection port, the high pressure area also distributes in the mold on both sides of the border, where air traps happen.

According to the pressure distribution results to adjust the export size and position, other factors do not make changes. Figure 11 shows the difference after changing. The simulation
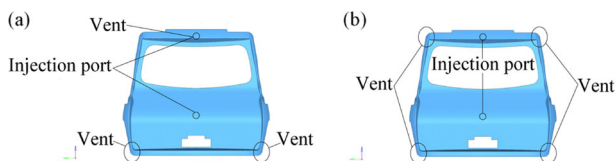

Fig. 11 Injection port and vent comparison before and after adjustment **a** before adjustment **b** after adjustment
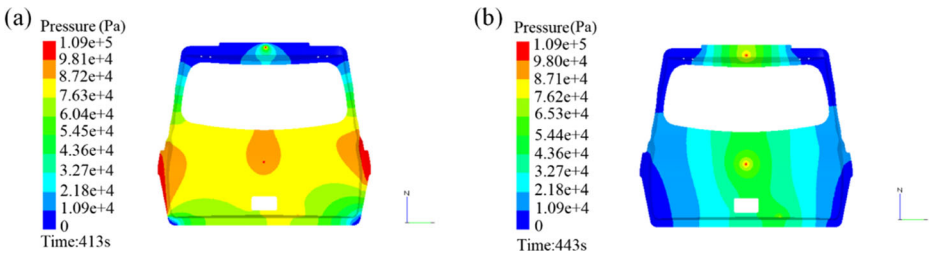
Fig. 12 Pressure distribution before and after adjustment **a** before adjustment **b** after adjustment

results are shown in Fig. 12. After the adjustment of the filling time, high pressure only exists in injection port. The air trap basically disappears and the forming quality can be guaranteed.

3.2.4 Performance Evaluation

The finite element model of the composite hatchback is reconstructed and analyzed in terms of torsion, bending and constraint modal subcase. Table 11 shows the performance comparison of DP 590 steel hatchback, initial composite hatchback and optimized composite hatchback. The results show that the optimized composite hatchback is 38.8% lighter than that of the steel hatchback, and the torsion, bending stiffness do not decrease. Comparing with initial composite hatchback, combinational optimization method results in better lightweight effect and avoids performance redundancy.

4 Conclusions

In this paper, an integrated design method combining "material – structure – process - performance" is proposed. Compared with MDO and KBE, This method achieves the iteration of "material – structure – process - performance" in the design process, and takes the interaction among these four factors into account to obtain the integrated design of the composite laminate component.

The method has been verified by a case of SUV composite hatchback design. The mass of final optimized composite hatchback reduces 38.8% compared with original steel one. The torsion stiffness, bending stiffness and first-order constraint modal frequency increase 3.75%, 33.23% and 44.78%, respectively.

The proposed method is also suitable for other composite components, which has a solid theoretical foundation.

Table 11 Performance comparison of steel hatchback, initial and optimized composite hatchback

Performance	DP 590 steel hatchback	Initial composite hatchback	Optimized composite hatchback
Torsion angle in subcase 1 (°)	0.133	0.069	0.128
Deflection in subcase 2 (mm)	0.710	0.406	0.474
1st modal frequency in subcase 3 (Hz)	27.4	45.9	39.67
Mass (kg)	12.26	8.55	7.50

References

1. Solazzi, L., Scalmana, R.: New design concept for a lifting platform made of composite material. Appl. Compos. Mater. **20**, 615–626 (2013)
2. Cao, S., Zhis, W.U., Wang, X.: Tensile properties of CFRP and hybrid FRP composites at elevated temperatures. J. Compos. Mater. **43**, 315–330 (2009)
3. Kim, P.: A comparative study of the mechanical performance and cost of metal, FRP, and hybrid beams. Appl. Compos. Mater. **5**, 175–187 (1998)
4. Yuan, C., Bergsma, O., Koussios, S., Zu, L., Beukers, A.: Optimization of sandwich composites fuselages under flight loads. Appl. Compos. Mater. **19**, 47–64 (2012)
5. Liu, T.J.C., Wu, H.C.: Fiber direction and stacking sequence design for bicycle frame made of carbon/epoxy composite laminate. Mater. Des. **31**, 1971–1980 (2010)
6. Pohlak, M., Majak, J., Karjust, K., Küttner, R.: Multi-criteria optimization of large composite parts. Compos. Struct. **92**, 2146–2152 (2010)
7. Gnädinger, F., Karcher, M., Henning, F., Middendorf, P.: Holistic and consistent design process for hollow structures based on braided textiles and RTM. Appl. Compos. Mater. **21**, 541–556 (2014)
8. Gandhi, U., Song, Y.Y., Mandapati, R.: Semiempirical approach to predict shrinkage and warpage of fiber-reinforced polymers using measured material properties in finite element model. J. Thermoplast. Compos. Mater. **30**, 1303–1319 (2017)
9. Gantois, K., Morris, A.J.: The multi-disciplinary design of a large-scale civil aircraft wing taking account of manufacturing costs. Struct. Multidiscip. Optim. **28**, 31–46 (2004)
10. Olson, G.B.: Computational design of hierarchically structured materials. Science. **277**, 1237–1242 (1997)
11. Grujicic, M., Arakere, G., Sellappan, V., Ziegert, J.C., Schmueser, D.: Multi-disciplinary design optimization of a composite car door for structural performance, NVH, crashworthiness, durability and manufacturability. Multidiscip. Model. Mater. Struct. **5**, 1–28 (2009). https://doi.org/10.1108/15736105200900001
12. Zhang, C., Kang, N., Li, L.J., Sun, L.Y.: Case Study: 'Material-Structure-Process-Performance' Integration Design and Numerical Verification of Automotive Composite Components. International Mechanical Engineering Congress and Exposition (ASME), Tampa (2017)
13. Wang, H., La Rocca, G., van Tooren, M.J.L.: A KBE–Enabled Design Framework for Cost/Weight Optimization Study of Aircraft Composite Structures. AIP Conference Proceedings (AIP), Louisiana (2014)
14. Choi, J.W., Kelly, D., Raju, J.: A knowledge-based engineering tool to estimate cost and weight of composite aerospace structures at the conceptual stage of the design process. Aircr. Eng. **79**, 459–468 (2007)
15. McDowell, D.L.: Simulation-assisted materials design for the concurrent design of materials and products. JOM. **59**, 21–25 (2007)
16. Marom, G., Fischer, S., Tuler, F.R., Wagner, H.D.: Hybrid effects in composites: conditions for positive or negative effects versus rule-of-mixtures behaviour. J. Mater. Sci. **13**, 1419–1426 (1978)
17. Chamis, C.C.: Mechanics of composite materials: past, present, and future. J. Compos. Technol. Res. **11**, 3–14 (1989)
18. Kalamkarov, A. L., Kolpakov, A.G.: Analysis, Design, and Optimization of Composite structures. Wiley, New York (1997)
19. Trochu, F., Ruiz, E., Achim, V., et al.: New Approaches to Accelerate Calculations and Improve Accuracy of Numerical Simulations in Liquid Composite Molding. International Conference on Flow Processes in Composite Materials (FPCM), Delaware (2004). https://www.fose1.plymouth.ac.uk/sme/fpcm/fpcm07/Extended_abstracts/EA255.pdf
20. Zhou, J., Sancaktar, E.: Chemorheology of epoxy/nickel conductive adhesives during processing and cure. J. Adhes. Sci. Technol. **22**, 957–981 (2008)
21. Kamal, M.R., Sourour, S.: Kinetics and thermal characterization of thermoset cure. Polym. Eng. Sci. **13**, 59–64 (1973)
22. Daniel, I.M., Ishai, O., Daniel, I.M., et al.: Engineering Mechanics of Composite Materials. Oxford University Press, New York (1994)

23. Suresh, S., Sujit, P.B., Rao, A.K.: Particle swarm optimization approach for multi-objective composite box-beam design. Compos. Struct. **81**, 598–605 (2007)
24. Marklund, P.O., Nilsson, L.: Optimization of a car body component subjected to side impact. Struct. Multidiscip. Optim. **21**, 383–392 (2001)
25. Kodiyalam, S., Yang, R.J.: Optimization of car body under constraints of noise, vibration, and harshness (NVH), and crash. Struct. Multidiscip. Optim. **22**, 295–306 (2001)
26. Craig, K.J., Stander, N., Dooge, D.A., Varadappa, S.: Automotive crashworthiness design using response surface-based variable screening and optimization. Eng. Comput. **22**, 38–61 (2005)
27. Bendsøe, M.P., Kikuchi, N.: Generating optimal topologies in structural design using a homogenization method. Comput. Methods Appl. Mech. Eng. **71**, 197–224 (1988)
28. Trochu, F., Gauvin, R., Gao, D.M.: Numerical analysis of the resin transfer molding process by the finite element method. Adv. Polym. Technol. **12**, 329–342 (1993)